



## Views &amp; Comments

# Constructing an Automation Table for an Image-Based *Arabidopsis* Resistance Assay



Goldi Makhija<sup>a,c</sup>, Dinesh S. Pujara<sup>b</sup>, In-Hyouk Song<sup>a</sup>, Byoung Hee You<sup>a</sup>, Hong-Gu Kang<sup>b</sup>

<sup>a</sup> Department of Engineering Technology, Texas State University, San Marcos, TX 78666, USA

<sup>b</sup> Department of Biology, Texas State University, San Marcos, TX 78666, USA

<sup>c</sup> Caresoft Global Inc., Burr Ridge, IL 60527, USA

## 1. Introduction

Crop improvement is becoming critical for food security due to a continuously changing climate and increasing population [1]. The management of plant diseases is one of the most important factors in food security. For example, wheat, a major crop plant, has been historically subject to periodic total devastation. In a recent instance, when a new strain of wheat stem rust spread from East Africa to the Middle East, the price of wheat spiked significantly, threatening livelihoods in developing countries [2]. This example highlights the importance of learning how plants fend off potential pathogens and pests, in order to secure food resources.

Identification of resistance traits has been one of the main tools in plant disease management [3]. For example, a long list of *R* (resistance) genes effective against disease in plants has been characterized and utilized for crop protection [4]. While these *R* genes trigger strong defense responses in response to infection from a wide range of pathogens and pests, the underlying signaling network, although highly complicated, appears to involve many common players. *Arabidopsis* non-expressor of PR (*NPR1*) gene, for example, has been shown to be a receptor for salicylic acid (SA), a well-known defense hormone [5], and is required for a majority of *R* gene-mediated resistance mechanisms [6]. Lack of *NPR1* leads to susceptibility to pathogens in not only *Arabidopsis* but also diverse plant species [7]. Many defense signaling components in *Arabidopsis* also play an important role in crop plants, which highlights the importance of characterizing the resistance signaling pathways in *Arabidopsis* in detail [8]. Unfortunately, as the number of these defense components increases, it becomes more difficult to characterize all the necessary genetic backgrounds due to the lack of affordable phenomics tools which can automate high-throughput plant resistance assays.

The increasing number of genetics resources, including natural and artificial variations, presents a valuable opportunity to identify important agronomic traits [9]. While large-scale genotyping is now routinely performed thanks to advances in sequencing technology, high-throughput phenotyping assays are far from routine because there are no fixed procedures and very few affordable phe-

nomics tools [10]. A resistance assay in plants is even more challenging in a high-throughput setup, since resistance traits are mostly assessed by quantitating infecting pathogens/pests through labor-intensive steps. To overcome these hurdles, a *Pseudomonas syringae* (*P. syringae*) strain was engineered to carry a luminescent reporter gene and used in the noninvasive imaging of infected leaves in order to quantitate resistance in plants [11]. This reporter strain allowed the assessment of over 100 *Arabidopsis* ecotypes, which led to the identification of two quantitative trait loci linked to the variance of basal bacterial resistance in *Arabidopsis* [11].

Automation is a critical element in high-throughput phenotyping, which is often accomplished by an automation table. Phenoscope and PHENOPSIS [12,13] are two commercial automation tables used in large-scale phenotyping. However, this type of automation tool is out of reach for traditional laboratories due to its high cost, which presents a major challenge for a large-scale study. To overcome this hurdle, we built an affordable automation table synchronized with a camera for large-scale image-based resistance analysis, which demonstrates the benefit of automation in one of the challenging areas in plant phenomics.

## 2. Methodology

### 2.1. Parts for the automation table

The automation table was assembled using the parts listed in Tables 1 and 2. A step-by-step assembly is described in the results section.

### 2.2. Programming code for synchronizing the automation table with an electron-multiplication charge-coupled device camera

A programming code written in C++ that was used to synchronize the automation table with an electron-multiplication charge-coupled device (EMCCD) camera is provided in Supplementary data in Appendix A.

**Table 1**  
Mechanical parts used to make an assembly for the x-axis.

Part name	UPC	Quantity
Nylon insert hex locknut–M5	819368021110	3
Aluminum spacer (6 mm)	819368021349	2
Aluminum spacer (40 mm)	819368021325	3
Low profile screws M5 (40 mm)	819368022063	4
1/4" × 8 mm flexible coupling	819368020915	1
Aluminum spacer (3 mm)	819368021349	4
Eccentric spacer (6 mm)	819368021011	2
Xtreme solid V wheel kit	819368020809	4
Spacer block	819368021691	2
V-Slot® gantry plate universal	81936802530	1
Self-tapping screw	819368021134	4
Low-profile screws M5 (55 mm)	819368021820	3
Ball bearing 688Z 8 mm × 16 mm × 5 mm	819368021028	2
Shim–12 mm × 8 mm × 1 mm	819368020700	2
Lock collar (8 mm)	819368020991	2
Threaded rod plate NEMA 23 stepper motor	819368021769	2
Low-profile screws M5 (15 mm)	819368021820	6
Anti-backlash nut block for 8 mm metric acme lead screw	819368021806	1
NEMA 23 stepper motor	819368021271	1
V-Slot® 20 × 60 linear rail (1000 mm)	819368020434	1
8 mm metric acme lead screw (290 mm)	819368020342	1

**Table 2**  
Electronic parts used to control the automation table.

Part type	Part brand and model	Quantity
Power supply	Eagwell 24 V 15 A DC universal regulated switching power supply	1
Stepper motor driver	SainSmart CNC router single 1 axis 3.5 A TB6560 stepper stepping motor driver board	2
Arduino controller	Arduino mega 2560 REV3	1
LCD control	SunFounder IIC I2C TWI 1602 serial LCD module display for Arduino uno R3 mega 2560 16 × 2	1

CNC: computer numerical control; DC: direct current; LCD: liquid crystal display.

### 2.3. Plant growth, bacterial infection, and quantitation of bacterial growth

*Arabidopsis* plants were grown in soil at 22 °C and 60% relative humidity, with a 16 h light period. Four-week-old plants were hand infiltrated using a needleless syringe at an indicated inoculum (in 10 mmol·L<sup>-1</sup> MgCl<sub>2</sub>) of *P. syringae* grown for 2 d at 28 °C in King's B medium with appropriate antibiotics. Inoculated leaves were harvested at the given time points, and then used for bacterial titer determination, as previously described [14].

### 2.4. In planta NanoLuc reporter assay

An EMCCD camera (C9100-23B, Hamamatsu, Japan) run by HCLImageLive software (Hamamatsu, Japan) was used to capture chemiluminescence from infected plants. The external edge trigger mode feature was used to synchronize the automation table. Prior to imaging, plants were placed in the dark for 30 min to reduce background luminescence. Infected leaves were sprayed with NanoGlo reagent (Promega, USA) and images were captured; the camera was set at a binning of 4 and a sensitivity gain of 297, with the photon imaging mode (PIM) activated at 1 and an exposure time of 1 min.

## 3. Assembly and a running example of the automation table

Our automation table was designed to move a traditional *Arabidopsis* flat, also known as a 1020 greenhouse tray, which holds

18 pots of *Arabidopsis* plants. We describe the assembly of the automation table in two sections: ① the mechanical section and ② the electronic section.

### 3.1. Assembly of the automation table: The mechanical section

High stiffness and thrust are necessary aspects of an automation table in order to support and move the weight of 18 pots. Precision is also crucial in order to consistently capture images. To achieve these requirements, a predesigned kit—the V-Slot® NEMA 23 linear actuator bundle (lead screw) with SKU number 1170-bundle and UPC number 819368022902—was used to provide a translation of the automation table along the x-axis. As shown in Fig. 1(a), the kit has a stepper motor, a lead screw, nuts, spacers, bearings, and a V-Slot® gantry plate. The movement is driven by the lead screw, and its motion is controlled by the stepper motor.

Each plant on the flat was located directly under the camera in order to capture its image. This positioning required translational movements of the table along both the x- and y-directions. A replica of the previously described linear bundle was positioned inversely on top of the x-axis. The x- and y-axes were assembled using the V-Slot® gantry plates of each axis, as shown in Fig. 1(b). An *Arabidopsis* tray cannot be placed directly on the designed assembly shown in Fig. 1(b) because its own weight would cause misalignment between the camera and the plants. Two V-Slot® linear rails were therefore mounted on the top of the assembly, as shown in Fig. 1(c), in order to keep the *Arabidopsis* tray stable and balanced during movement.

Fig. 1(d) shows a three-dimensional solid model of the automation table supporting 18 *Arabidopsis* pots. This table was capable of driving the plants smoothly, despite the considerable weight of the soil and water (see [Supplementary video in Appendix A](#)). A generic photo station was used to fix the camera, whose height could be manually adjusted (Fig. 1(e)). The automation table was placed under the camera.

### 3.2. Assembly of the automation table: The electronic section

Two NEMA 23 stepper motors were used to drive the x- and y-axes of the automation table. A micro-controller—the SainSmart computer numerical control (CNC) router single 1 axis 3.5 A TB6560 stepper stepping motor driver board—was used to provide electrical pulses to the motor, and the pulses were amplified using a direct-current (DC) power supply. A liquid crystal display (LCD) was included to indicate the live location of the plants on the flat. All components were electrically connected, as shown in Fig. 2. The Arduino controller stored the entire logic of the operation for image capturing, and provided the necessary sequences of electric pulses to the stepper motors accordingly. It also triggered the camera at the desired moment and controlled the LCD to display the location of the table.

### 3.3. Image-based resistance assay facilitated by the automation table

We have recently developed a *P. syringae* strain (manuscript under preparation) carrying one of the brightest luminescence reporters, NanoLuc Luciferase [15], for image-based resistance assay in plants. To test whether the automation table could facilitate this image-based assay, we infected *Arabidopsis* plants with the luminescent *P. syringae* and imaged them as they were mobilized by the automation table. An EMCCD camera imaged these infected plants nine consecutive times with no interruption. It should be noted that *Arabidopsis* plants that had been infected with the luminescent *P. syringae* for 1, 2, and 3 d were imaged (Fig. 3). A representative picture from each different time is shown

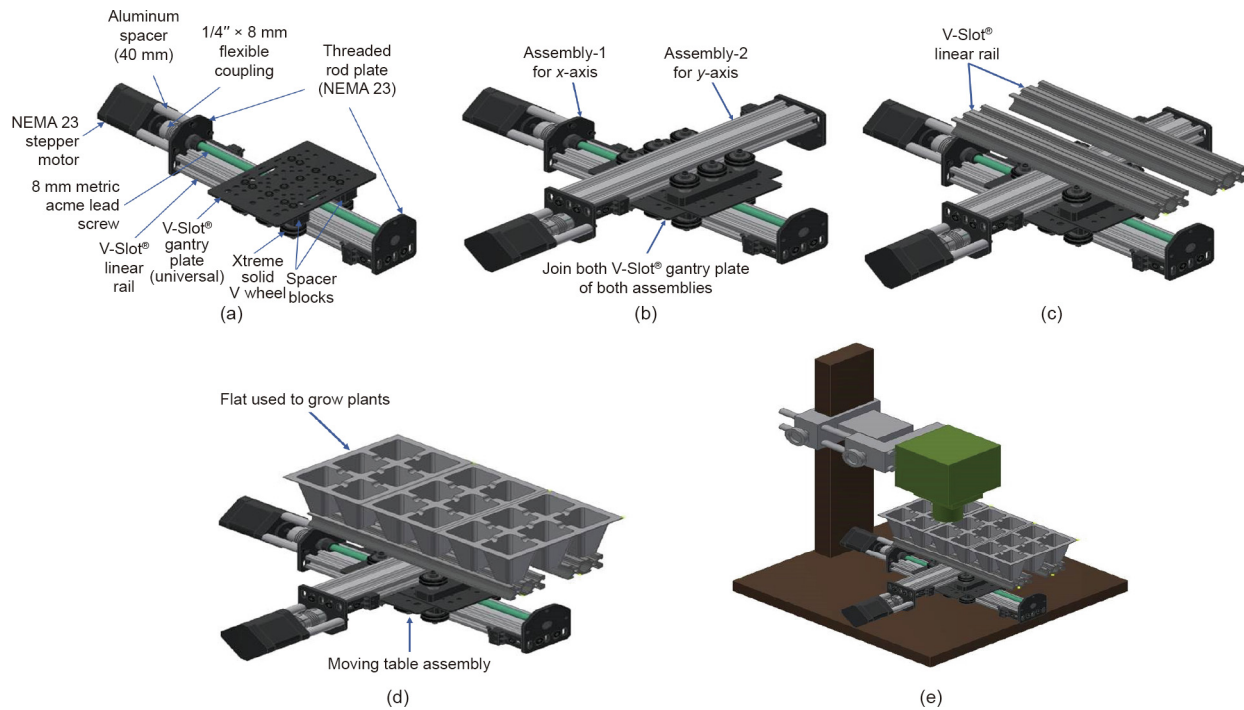


**Fig. 1.** Automation table assembly with a camera and its stand. Two motor-controlled rails were placed to control two-dimensional movements. Once (a) the first rail was assembled, (b) the second rail was placed on the top. (c) A mounting rail was used to support, (d) a plant growth flat. (e) The assembled table was placed under an electron-multiplying charged coupled device (EMCCD) camera.

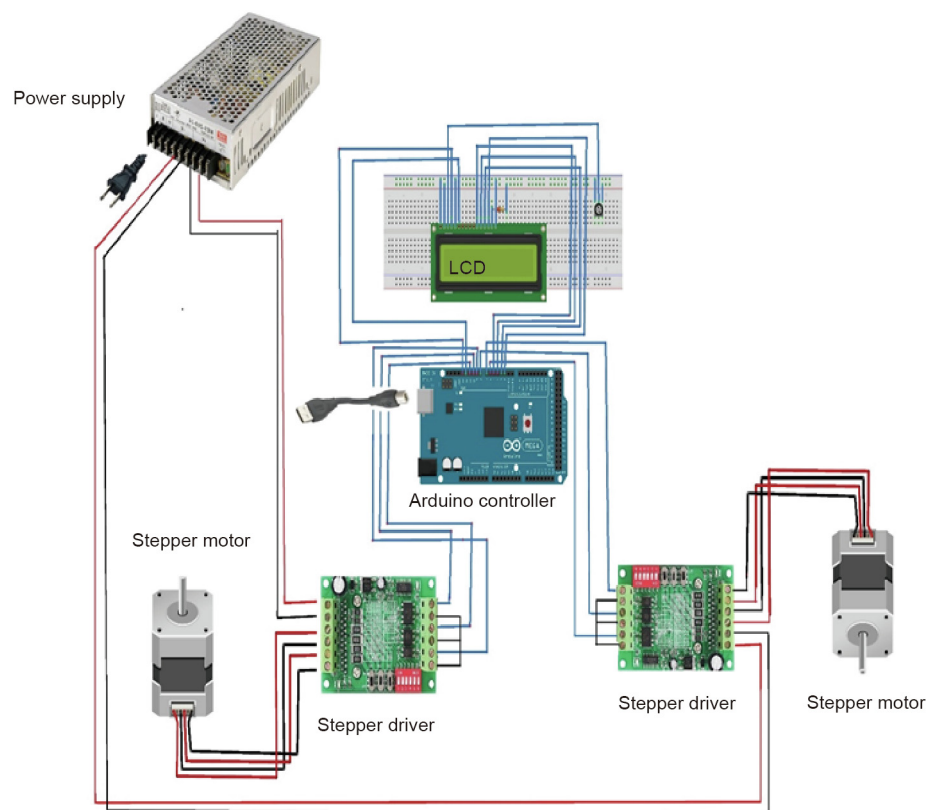


**Fig. 2.** The physical connection of each electronic component involved in moving the assembly.

in Fig. 3(b). To ensure that this image-based resistance assay was as quantitative as its conventional counterpart, values from two methods were plotted, as shown in Fig. 3(b), which revealed a

strong linear correlation. These outcomes suggest that the image-based assay aided by the automation table produced highly quantitative data with minimum manual input.

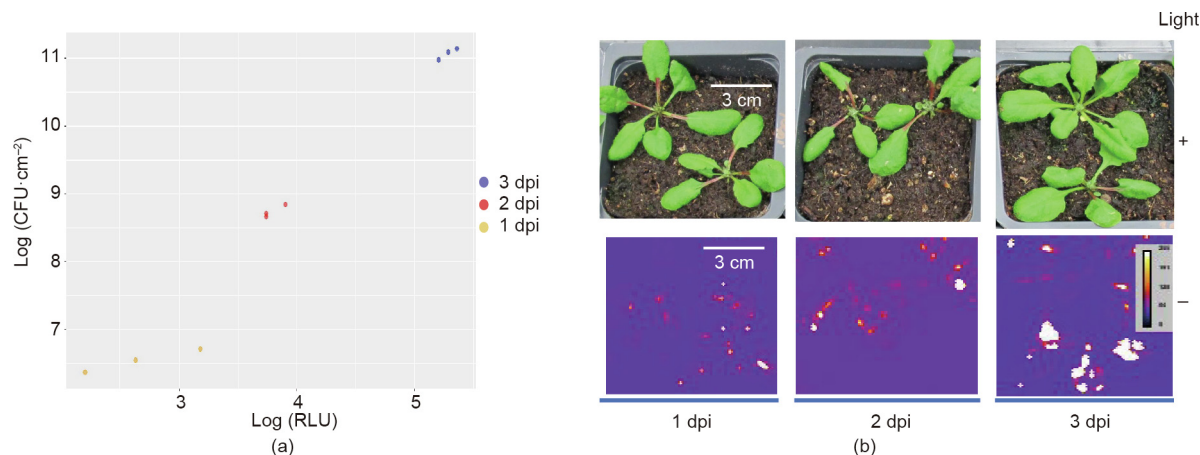


**Fig. 3.** The image-based resistance assay coupled with the automation table produced quantitation data that was comparable to its conventional counterpart. (a) Correlation between the image-based (x-axis) and conventional (y-axis) assays. 3.5-week-old *Arabidopsis* plants were syringe infiltrated with  $10^5$  CFU mL<sup>-1</sup> of luminescence-tagged *P. syringae*. The infected plants at the indicated day post infection (dpi) were sprayed with the NanoGlo substrate and imaged using an EMCCD camera as shown in the x-axis. The same infected leaves were subject to a conventional leaf grinding assay in which a bacterial titer was measured as shown in the y-axis. (b) Representative pictures with and without light. Luminescence from infected plants, which was taken without light, is shown in pseudo-color for better differentiation. CFU: colony-forming unit; RLU: relative light unit.

#### 4. Concluding remarks and perspectives

We have developed a custom-made automation table that facilitates high-throughput resistance assays. The table has two motor-controlled T-slot metal bars. The movement is synchronized with an EMCCD camera, which permits the uninterrupted imaging of plants. This automation tool, in combination with a recently developed luminescent *P. syringae* strain, allowed the resistance analysis of more than 30 infected *Arabidopsis* plants in less than 10 min. If performed manually, the same resistance assay would generally take several hours, as it involves several labor-intensive steps.

Our image-based resistance analysis for plants utilizes an EMCCD camera, which captures images from dim luminance. This high-throughput-friendly method, when combined with the automation table, was performed at arguably the shortest time for plant resistance analysis to date (less than a few minutes versus several hours). In addition to its role in enhancing high throughput, this fast speed offers additional benefits to an EMCCD camera equipped with a highly sensitive imaging sensor that is designed to amplify a very dim light signal. The sensitivity of the EMCCD camera degrades over time, in a process known as gain aging, which leads to poor sensor sensitivity [16]. Severe gain aging makes an EMCCD camera unusable for image-based resistance assays, and it is very expensive to repair this aging issue based on our experience. Imaging with no interruption using an automation table provides the shortest possible running time, in addition to reducing unnecessary exposure to room lights due to occasional user errors, and will therefore help to maintain the high sensitivity of the camera for a longer time.

Plant defense signaling has been intensively studied, resulting in the identification of many well-defined signaling pathways [17]. As more and more defense signaling components are characterized, the need to analyze a larger set of plants continues to grow. However, a conventional resistance assay, which relies on the manual counting of pathogens, is not generally conducive to a high-throughput experimental setting. The focus of individual studies has therefore been on changes in resistance in a few genetic backgrounds. For the same reason, the resistance trait distribution within a genetically homogeneous line has rarely been measured. It is increasingly apparent that the eukaryotic genome is highly dynamic, particularly under stress [18,19]. One of the contributing factors in this dynamicity is

the increased activity of transposable elements, which can change the genome [20]. Thus, we envision that, once a large-scale resistance study becomes the norm in the field of plant pathology, an interplay among the defense signaling factors and even resistance variance within a homologous genetic background would be uncovered.

The automation table presented in this study accommodates a conventional *Arabidopsis* tray. This table can easily be up-scalable by replacing a bar and a motor with others having adequate capacity. Most laboratories have limited options for automation when it comes to imaging plants on a large scale. Although advanced automation tools have great potential to enhance phenotyping capabilities, low-cost and/or do-it-yourself (DIY) phenotyping solutions such as the automation table presented in this study will reduce the entry barrier [21], which will further popularize a high-throughput approach. Therefore, we hope that our affordable automation table will encourage more laboratories to commit to large-scale resistance assays in order to better characterize ever-complicating plant defense signaling.

#### Acknowledgements

We thank Angela H. Kang for critical comments on this manuscript and John Word for feedback/help on designing the automation table. This work is supported by the National Science Foundation (IOS-1553613 to Hong-Gu Kang).

#### Appendix A. Supplementary data

Supplementary data to this article can be found online at <https://doi.org/10.1016/j.eng.2019.09.009>.

#### References

- [1] Tester M, Langridge P. Breeding technologies to increase crop production in a changing world. *Science* 2010;327(5967):818–22.
- [2] Soko T, Bender CM, Prins R, Pretorius ZA. Yield loss associated with different levels of stem rust resistance in bread wheat. *Plant Dis* 2018;102(12):2531–8.
- [3] Bent AF, Mackey D. Elicitors, effectors, and R genes: the new paradigm and a lifetime supply of questions. *Annu Rev Phytopathol* 2007;45:399–436.
- [4] Martin GB, Bogdanove AJ, Sessa G. Understanding the functions of plant disease resistance proteins. *Annu Rev Plant Biol* 2003;54:23–61.



- [5] Wu Y, Zhang D, Chu JY, Boyle P, Wang Y, Brindle ID, et al. The *Arabidopsis* NPR1 protein is a receptor for the plant defense hormone salicylic acid. *Cell Rep* 2012;1(6):639–47.
- [6] Withers J, Dong X. Posttranslational modifications of NPR1: a single protein playing multiple roles in plant immunity and physiology. *PLoS Pathog* 2016;12(8):e1005707.
- [7] Fu ZQ, Dong X. Systemic acquired resistance: turning local infection into global defense. *Annu Rev Plant Biol* 2013;64:839–63.
- [8] Piquerez SJ, Harvey SE, Beynon JL, Ntoukakis V. Improving crop disease resistance: lessons from research on *Arabidopsis* and tomato. *Front Plant Sci* 2014;5:671.
- [9] Unamba CI, Nag A, Sharma RK. Next generation sequencing technologies: the doorway to the unexplored genomics of non-model plants. *Front Plant Sci* 2015;6:1074.
- [10] Houle D, Govindaraju DR, Omholt S. Phenomics: the next challenge. *Nat Rev Genet* 2010;11(12):855–66.
- [11] Fan J, Crooks C, Lamb C. High-throughput quantitative luminescence assay of the growth in planta of *Pseudomonas syringae* chromosomally tagged with *Photobacterium luminescens luxCDABE*. *Plant J* 2008;53(2):393–9.
- [12] Tisné S, Serrand Y, Bach L, Gilbault E, Ben Ameer R, Balasse H, et al. Phenoscope: an automated large-scale phenotyping platform offering high spatial homogeneity. *Plant J* 2013;74(3):534–44.
- [13] Granier C, Aguirrezabal L, Chenu K, Cookson SJ, Dauzat M, Hamard P, et al. PHENOPSIS, an automated platform for reproducible phenotyping of plant responses to soil water deficit in *Arabidopsis thaliana* permitted the identification of an accession with low sensitivity to soil water deficit. *New Phytol* 2006;169(3):623–35.
- [14] Kang HG, Kuhl JC, Kachroo P, Klessig DF. CRT1, an *Arabidopsis* ATPase that interacts with diverse resistance proteins and modulates disease resistance to turnip crinkle virus. *Cell Host Microbe* 2008;3(1):48–57.
- [15] Hall MP, Unch J, Binkowski BF, Valley MP, Butler BL, Wood MG, et al. Engineered luciferase reporter from a deep sea shrimp utilizing a novel imidazopyrazinone substrate. *ACS Chem Biol* 2012;7(11):1848–57.
- [16] Dunford A, Stefanov K, Holland A. Ageing and proton irradiation damage of a low voltage EMCCD in a CMOS process. *J Instrum* 2018;13:c02059.
- [17] Ramirez-Prado JS, Abulfaraj AA, Rayapuram N, Benhamed M, Hirt H. Plant immunity: from signaling to epigenetic control of defense. *Trends Plant Sci* 2018;23(9):833–44.
- [18] Bordiya Y, Zheng Y, Nam JC, Bonnard AC, Choi HW, Lee BK, et al. Pathogen infection and MORC proteins affect chromatin accessibility of transposable elements and expression of their proximal genes in *Arabidopsis*. *Mol Plant-Microbe Interact* 2016;29(9):674–87.
- [19] Lapp HE, Hunter RG. The dynamic genome: transposons and environmental adaptation in the nervous system. *Epigenomics* 2016;8(2):237–49.
- [20] Huang CR, Burns KH, Boeke JD. Active transposition in genomes. *Annu Rev Genet* 2012;46:651–75.
- [21] Roitsch T, Cabrera-Bosquet L, Fournier A, Ghamkhar K, Jiménez-Berni J, Pinto F, et al. Review: new sensors and data-driven approaches—a path to next generation phenomics. *Plant Sci* 2019;282:2–10.